Desalination and Water Treatment
www.deswater.com

doi: 10.1080/19443994.2016.1180480

57 (2016) 23119–23131
October

Taylor & Francis
Taylor & Francis Group

A transient model for forward and parallel feed MED

Marios C. Georgiou*, Aristides M. Bonanos

Energy Environment and Water Research Center, The Cyprus Institute, Nicosia 2121, Cyprus, Tel. +357 22 208 604; Fax: +357 22 208 625; emails: m.c.georgiou@cyi.ac.cy (M.C. Georgiou), bonanos@cyi.ac.cy (A.M. Bonanos)

Received 4 May 2015; Accepted 3 March 2016

ABSTRACT

The aim of this paper is to investigate the performance of a multiple effect distillation (MED) unit potentially coupled to a concentrated solar power plant and validate the results with the predictions of a dynamic model that was developed for this purpose. A small-scale (10 $kW_{thermal}$) four effect distillation system was designed and built to demonstrate proof of principle of the concentrating solar power–desalinating sea water system integration. In order to fully characterize this small-scale MED unit, an understanding of the performance for steady state and transient conditions is required. Initially experiments were performed in a steady state situation, various parameters were examined and the experimental findings have already been published. After the initial experimental findings of the steady state operation, the performance of this unit was also investigated for transient conditions. The experimental procedure followed was identical as in the steady state conditions, with the main difference being the variation in the heat input supply to the system as a function of time. For the present study, the heat input supplied to the unit varied between 5 and 10 $kW_{thermal}$. At the same time, a dynamic model was also developed in order to predict the performance of this unit in consecutive time steps of operation. The performance was calculated in terms of performance ratio (the ratio of the distillate product flow rate to the feeding steam flow rate) and the model results were validated against the experimental findings. The results showed that there is a really good match between the experimental data and the predicted ones from the model.

Keywords: Desalination; Multiple effect distillation (MED); Transient operating conditions; Dynamic model

1. Introduction

Throughout humanity's history and especially within the last decades, water and energy topics are two of the most crucial ones. These parameters though are closely related: the production of energy requires water, whilst the treatment and distribution of water are dependent on energy [1].

Especially for the Mediterranean and the Middle East regions where many cities and villages are already facing water shortage problems and suffer from lack of quality fresh water resources, the challenges are even bigger. Additionally, environmental

*Corresponding author.

Presented at EuroMed 2015: Desalination for Clean Water and Energy Palermo, Italy, 10–14 May 2015. Organized by the European Desalination Society.

considerations, such as the proven global warming and climate change, will surely add significant pressure to the existing crisis [2].

At the same time, the above-mentioned areas are blessed with high solar potential that can reach up to 2.700 kW_h/m^2 per year. Despite the additional stress that the intense solar radiation imposes on the scarce water resources, it can be exploited as the medium to reverse the crisis. Renewable energy sources (RES) are rapidly increasing their contribution to the total energy mix and this increasing trend is expected to continue in the upcoming future [3,4]. Among the various RES, solar energy has the greatest potential and taken into account that areas where there is water stress situation are also blessed with intense solar radiation the outcome is that technologies capable of using the solar energy should be developed in order to simultaneously help solve energy and water problems [5].

Several researchers have considered the driving of desalinating systems with RES and specifically the coupling of desalination processes with solar energy. The selection of the appropriate RES desalination technology relies on a variety of factors such as: the plant size, the feed water salinity, the shoreline distance from the plant and the type and potential of the local renewable energy resource [6–8]. The characteristics of the system that will be implemented for the RES desalination are: simplicity of operation, low maintenance, robustness and autonomous operation. The most important characteristic should be its stable operation even when sudden changes are made and its ability to follow a varying steam supply without upset.

This paper investigates the performance of a desalination unit coupled with solar thermal energy, and considers the units operation under time varying input conditions due to the variation in the primary energy source. The performance of a small-scale four effect multiple effect distillation (MED) unit has been evaluated and a dynamic model to predict the performance of the unit is developed and presented. The model is validated against the steady-state performance of the design and is used to predict the transient behaviour of the device.

2. The MED Process

Thermal desalination processes are based on evaporation–condensation process. As the name implies MED process consists of several consecutive stages called effects [9]. Each effect contains a multiphase heat exchanger. Seawater is introduced in the evaporator side and heating steam in the condenser side. As the seawater flows down the evaporator surface, part of it is evaporated, while the remainder collects at the bottom of each effect as brine. The pure water vapour raised by seawater evaporation at a lower temperature than the vapour in the condenser, due to the boiling point elevation (BPE) observed in saline solutions. However, it can still be used as heating medium for the next effect where the process is repeated. The decreasing pressure from one effect to the next one allows brine and distillate to be drawn to the next effect where they will flash and release additional amounts of vapour at low pressure. This additional vapour will condense into distillate inside the next effect. In the last effect, the produced steam condenses on a heat exchanger, called distillate or final condenser and, which is cooled by the seawater used in the first effect.

The MED process can be configured in forward, backward or parallel feed (PF) according to the flow directions of the brine [10]. In the forward feed (FF) configuration, the feed water stream flows to the first effect through the final condenser where it is heated by the condensing vapours produced in the final effect. At the same time, the brine from the previous effect is used as the feed water in the next effect. In the PF configuration, the feed water stream does not flow to the first effect via the final condenser as in the FF configuration but it is divided into multiple feed streams flowing to each effect in parallel [11].

3. Experimental set up

The experimental set up, schematic of which is shown in Fig. 1, consists of the following main components.

3.1. Hot steam supply

For the hot steam supply a steam generator machine was used. The Lavor GV 30 is a large capacity 30-kilowatt industrial steam generator, capable of producing steam within the range of 3.5–10 bar (145 psi) at maximum temperature of 180˚C. The operating principle is based on electric water heaters that are used to heat up the water up to the desired temperature and pressure. Due to the uninterrupted use of the machine, steam can be continuously provided to the first effect of the unit, in constant temperature and flow, therefore the operating conditions are normalized. With water tank capacity of 25 L, Lavor GV 30 can produce up to 37.5 kg of steam per hour.

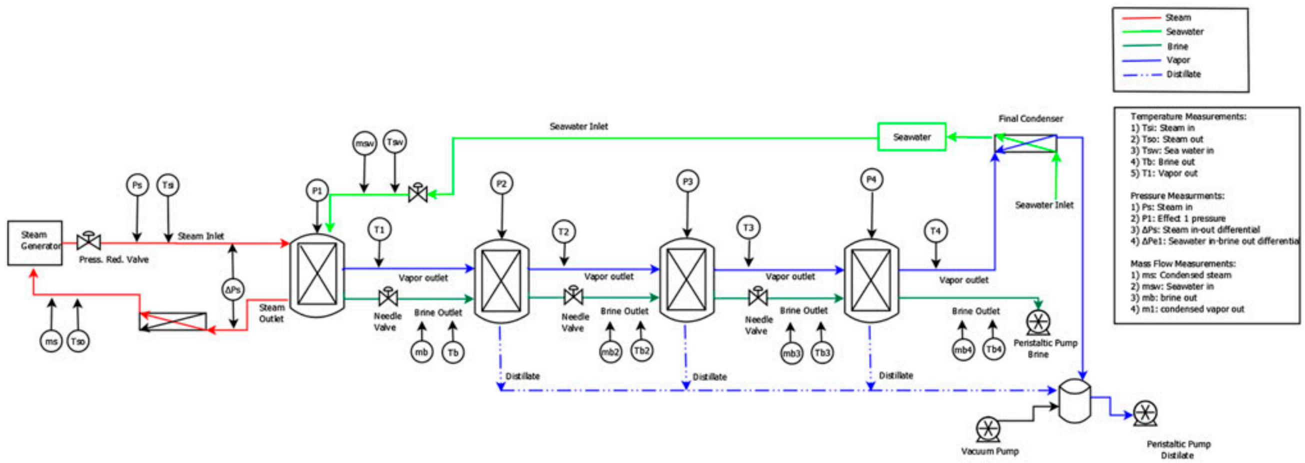

Fig. 1. Schematic of the experimental set up of the four effect distillation unit.

3.2. Feed water

The storage of feed water is done in plastic tanks placed outdoor, thus the feed water temperature was seasonal depending on the outdoor conditions. The capacity of the storage tanks is 2 tons thus there is sufficient amount of intake water for uninterrupted operating. Next to the tank, a water pump was placed in order to achieve higher water flows.

3.3. Vacuum pump

Additionally, a vacuum system was needed in order to remove the gases at the beginning of the experiment. An oil sealed rotary vane vacuum pump (Edwards RV 8) was used to maintain the gradual pressure gradient inside the vessel by removing the accumulated non-condensable gases together with the remaining water vapour after the final condensation stage. The pressure gradient along the MED effects was dictated by the saturation pressure of the feed stream and the saturation pressure of the condensing steam exiting the last effect and is condensed by the final condenser.

3.4. Evaporator/Condenser

One of the innovations of this small-scale unit was the usage of off-the-shelf components as many components traditionally used in MED are not commercially available in this scale. One of these components is the plate heat exchangers (PHEs) used as evaporators and condensers. The M3-FG seawater-compatible PHE, rated for up to 20 kW heat input, manufactured by Alfa Laval was selected. Plate falling film exchangers have been reported to exhibit evaporative heat transfer coefficients up to 4,000 W/m^2 K, and so are ideal for use in MED systems providing large heat transfer in compact areas. Modifications to the sealing gaskets to allow for three-phase flow were also made. The heat exchanger has a surface area of 0.353 m^2 comprised of 13 plates in an alternating pattern of alternating chevrons with 60° corrugation angle and fluid passage gap of 2.2 mm.

3.5. Auxiliary components

Auxiliary components include polypropylene pipes, peristaltic pumps to withdraw the brine and the distillate product, SS316 vessels, needle valves, and tanks for rejected brine and distillate product. These include tanks for supply, concentrate withdrawal and distillate receiver along with connecting pipes.

4. Measurements

A variety of parameters was acquired and monitored during the experiments. The parameters recorded, were: flow rate, pressure, and temperature of steam, seawater mass and temperature, brine mass and temperature, distillate product mass and water level within the vessel. Additionally, differential pressure transducers between the heat exchanger inlet and outlet on the steam and seawater sides measure the pressure drop across the condenser and evaporator, respectively.

Temperature, flow rate, pressure and differential pressure were measured at the locations shown in schematic, Fig. 2. Temperatures were measured K-type

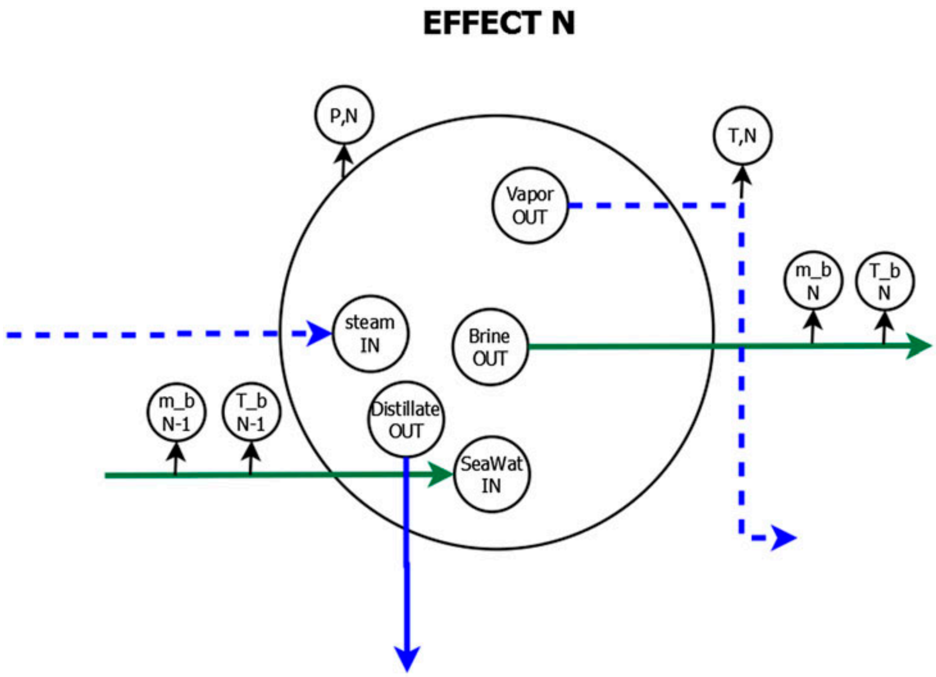

Fig. 2. Schematic of the location of several sensors placed for monitoring.

thermocouples calibrated with an ice point calibrator (Omega TRC-IIIA). Seawater and brine flow rates were measured using ultra-low flow sensors (Omega FTB600B Series). The pressure of the incoming steam and inside the effect was measured using pressure sensors (Omega PX209 Series) and the water level in the vessel was measured using a liquid level sensor (VEGACAL 63 of VEGA). All sensors were connected to a data acquisition system (DAQ) and LabView software was used to record the data.

5. Experimental process

The experimental process was as follows: initially, the unit was evacuated to remove all non-condensable gasses and then steam and seawater were allowed to flow. The start-up process lasted about one hour, during which time the pressure and the temperature of the system were gradually raised. Once a steady state was obtained, data acquisition commenced. A typical run lasted between 20 and 30 min, and consisted of recording effect temperature, pressure, flow rates and brine height level within the vessel. As mentioned above, temperatures were recorded using type-K thermocouples that were previously calibrated against a NIST traceable standard using an ice-point reference and an immersion heater, to reduce their error to ±0.4˚C in the 30–150˚C range. Subsequently, the parameter under investigation was varied and the process was repeated [12].

The aim during each run was to minimize the variation in flow properties and achieve a steady production of distillate. A statistical analysis was performed over all data samples gathered for a given run, and the variance and error were computed. Uncertainty analysis of measurements was conducted to establish a confidence in the measurements. A 95% confidence interval was used reflecting a significance level of 0.05.

It is important to note here again, that the objectives of the present study was to evaluate the performance of the multi effect distillation unit in terms of PR under various operating conditions thus the parameters examined are: the thermal input power, the seawater flow rate and temperature and the distribution of the seawater. The quality of the produced water, although a critical parameter of the complete MED unit, is not studied here but remains as an objective for future work.

Fig. 3 shows a representative time record of flow metre sensor outputs collected during the single-effect experiments. From the data collected it can be clearly seen, that there is a variation in the steam's flow rate (m_{st}), whereas in contrast the seawater (m_{sw}) and brine (m_b) flow rates are fairly steady. The variance of the steam flow rate is mainly caused by the temperature controller of the steam generator that creates a cyclical

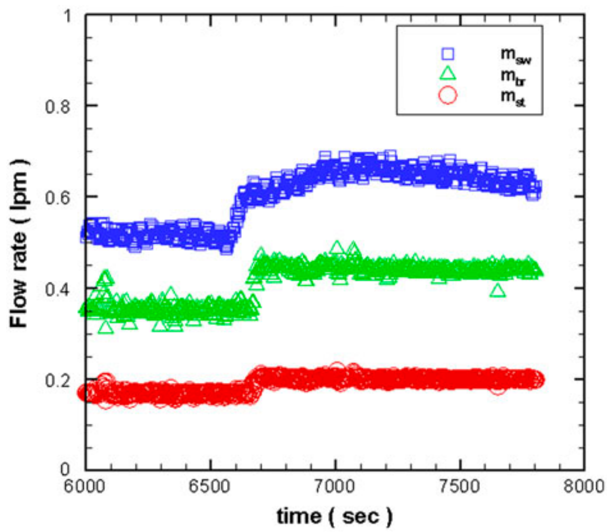

Fig. 3. Representative time record of flow metre sensor output collected from the single effect unit.

variation in its output flow rate. The fact though that the steam flow rate variation does not affect the operation of the effect is an indication of the robustness of the MED process.

The experimental unit developed and constructed for the purposes of this study is shown in Fig. 4.

6. Overview of the MED models in literature

The MED process is a well-known process proposed many decades ago, thus in the literature there are many mathematical models describing the performance of these units. These can be divided into two main categories:

(1) Steady state models.
(2) Dynamic models.

Despite the fact that most of the model widely used are steady state models, the limitations of these models lead to the introduction of new dynamic models in order to overcome these restrictions. Typically, steady state models are developed based on the specific MED plant configuration: FF, backward feed (BF), PF and parallel cross feed (PCF). At this point, it is worth noting that the amount of models dealing with FF configuration is significantly higher compared to the ones describing PF or BF, although the PF configuration is most employed in industry. On the other hand, regarding the available literature on dynamic modelling of MED system, unfortunately, very few papers can be found. However, the interest for this kind of modelling has grown recently.

6.1. Steady state models

The variety of the parameters affecting the performance of an MED unit are: the number of effects, the heating steam temperature, the heat transfer area (HTA), the intake seawater temperature (preheaters), the top boiling temperature (TBT) and the various configurations of the feed water, so as the implementation of thermal vapor compression (TVC) or mechanical vapor compression (MVC). Therefore, there are several models available approaching one or

Fig. 4. Photo of the four effect experimental unit.

more of these parameters and predicting the PR of the unit based on their initial assumptions.

The modelling of MED goes back to 1980, when one of the first models was developed in order to calculate the PR and the HTA of a FF-MED with flash evaporation [13]. Two decades later, a research group leader by Darwish et al. [14,15] investigated the performance of several MED units with respect to the feed configurations. Additionally to the parameter of the feed configuration, the implementation of TVC or MVC was also investigated. Their results showed that the parallel/cross feed MED system has the best performance. Despite that, due to the simplicity of the design and the operation of the PF, but also due to the similar performance the PF configuration was implemented by the industries as mentioned above. Furthermore, they also studied the effect of the steam temperature, the HTA and so as the increasing number of effects with respect to the PR of the unit.

A few years later, the same scientific group developed a MED model where they also analyzed the various feed configurations and discussed the correlation between PR and the HTA. Their findings were that for a temperature difference (ΔT) between effects of less than 2˚C the HTA will be significantly increased. Additionally two other individual researchers groups [16,17] examined the effect of the number of effects, the TBT, so as the seawater temperature of the unit as a function of the thermal performance and the PR, respectively. The outcome was that the PR increased with increasing number of effects while TBT and inlet seawater temperature have a reduced impact on plant performance [18]. The gain output ratio (GOR) of an MED (with and without TVC) as a function of number of effects and varying TBT was also examined [19]. The findings were that an increase in the number of effects from 3 to 6 resulted in an almost twofold increase in the GOR.

A more recent study, in 2008 [20], examined the HTA of a unit for a constant TBT. The results showed that at a same TBT (70˚C), a 32% increase in the condenser area would increase the unit production by a 15%. Last, a year later [21], another study was conducted in order to define the optimum performance of an MED unit based on the designed parameters. They concluded that optimum performance depends on an optimum number of effects which itself depends on sea water salinity, feed water temperature and temperature differences between effects.

6.2. Dynamic models

As mentioned in the introduction of this chapter, the available information regarding dynamic models is limited. In 1997 [22] one of the first dynamic models was developed to study the transient behaviour of the MED process. This model allowed the study of system start-up, shutdown, load changes and troubleshooting in which the plant performance changed significantly. Next, almost a decade later, in 2006 another dynamic simulator was proposed for a single effect of a MED—VC unit [23]. Later on, in 2012 [24] and 2015 [25,26], two more studies were conducted at CIEMAT-Plataforma Solar de Almería (PSA), the first one to describe the performance of a 14 FF-MED unit, and the last one to study the thermal dynamics of the heater and the distillate production rate of another FF-MED plant. Both of these studies used Modelica language for their simulations.

7. Model development

As mentioned in the previous sections a wide range of mathematical models for MED are well reported in the literature but not so extensive work has been done on the dynamic behaviour of MED systems. In the present study, dynamic behaviour of multi-effect evaporator system used for desalination purposes is obtained by disturbing the feed flow rate, feed concentration, steam temperature and feed temperature.

The approach followed during the development of this model, is similar with the ones referenced in the literature above. Similarly to the steady state models, energy and material balance equations were used for a number of variables such as for the feed, product and vapour flow. The novelty of the proposed model is the flexibility that it can be applied to all kind of feeding arrangements like FF, BF and cross/PF with simple modifications and it can be also applied for any number of effects. The final equations that arise through this model were solved using MATLAB solvers.

Following the approach typically used in the literature [27–29], the MED process is modelled as consisting of three lumps—those for the heat exchanger, the vapor within the effect and the brine—which interact by exchanging mass energy and salt content. These interactions used in the present model are shown in the typical control volume for the *i*th effect, Fig. 5.

The model is developed by applying the laws of conservation of mass, species (salinity) and energy to the three lumps.

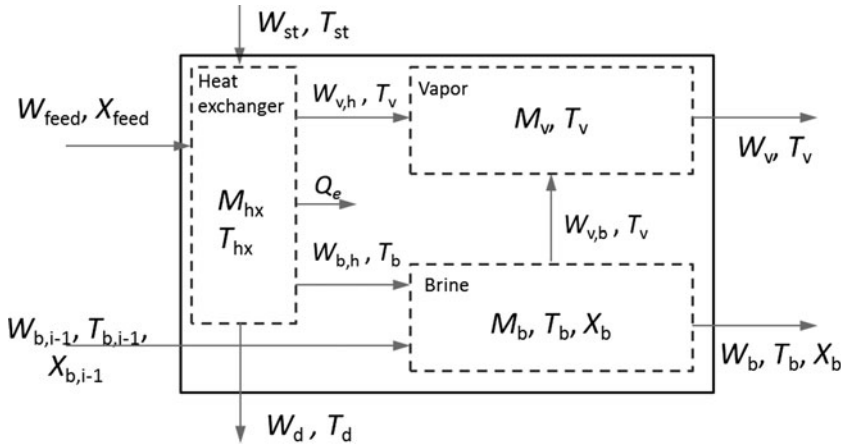

Fig. 5. Control volume used in model formulation.

7.1. Overall model assumptions

The model was based on the following assumptions:

(1) The vapor and liquid phase temperature in the evaporator are related to each other using the BPE relationship.

$$T_{\rm b} = T_{\rm v} + {\rm BPE}$$

(2) The lumps are considered well-stirred tanks, the temperature of the vapor leaving the evaporator is equal to the vapor temperature in the evaporator, and the temperature of the brine leaving the evaporator is equal to the pool brine temperature in the effect.
(3) Equal HTA for each effect is assumed.
(4) The thermophysical properties are taken as functions of temperature and salinity, as given in [30]. So, the derivative of the brine temperature with respect to time may be expressed as:

$$\frac{{\rm d}T_{\rm b}}{{\rm d}t} = \left(1 + \frac{\partial {\rm BPE}}{\partial T}\right)\frac{{\rm d}T}{{\rm d}t} + \frac{\partial {\rm BPE}}{\partial X}\frac{{\rm d}X}{{\rm d}t}$$

(5) The assumption that the heat exchanger is perfectly made, in other words all energy released by the condensing fluid is absorbed by the evaporating fluid.
(6) Additionally, the assumption that the mass of fluid within the heat exchanger does not change as a function of time is made.
(7) Finally, the heat exchanger is assumed to be at the same temperature as the effect, e.g. the thermal inertia of the heat exchanger is neglected.

7.2. Conservation of mass

Conservation of mass for brine, vapor and heat exchanger lumps gives:

$$\frac{{\rm d}M_{\rm b}}{{\rm d}t} = W_{{\rm b},i-1} + W_{\rm b,hx} - W_{\rm v,b} - W_{\rm b}$$

$$\frac{{\rm d}M_{\rm v}}{{\rm d}t} = W_{\rm v,hx} + W_{\rm b,hx} - W_{\rm v}$$

$$\frac{{\rm d}M_{\rm hx}}{{\rm d}t} = 0 = W_{\rm feed} - W_{\rm v,hx} - W_{\rm b,hx}$$

Substituting from the vapor and heat exchanger lumps into the brine, one can obtain:

$$\frac{{\rm d}M_{\rm b}}{{\rm d}t} = W_{\rm feed} + W_{{\rm b},i-1} - W_{\rm v} - W_{\rm b} - \frac{{\rm d}M_{\rm v}}{{\rm d}t}$$

Now, consider that $M = \rho AD$, where ρ is density, A is effect area and D is fluid level. Since the effect is a closed vessel of fixed height, the brine and vapor levels are related by $L_{\rm v} = H - L$, where L is the brine level and H is the height of the effect. Using this expression for the mass of brine, the derivative of $M_{\rm b}$ with respect to time may be calculated as:

$$\begin{aligned}\frac{{\rm d}M_{\rm b}}{{\rm d}t} &= \rho_{\rm b}A\frac{{\rm d}L}{{\rm d}t} + AL\frac{d\rho_{\rm b}}{{\rm d}t}\\ &= \rho_{\rm b}A\frac{{\rm d}L}{{\rm d}t} + AL\left(\frac{\partial\rho_{\rm b}}{\partial T_{\rm b}}\frac{{\rm d}T_{\rm b}}{{\rm d}t} + \frac{\partial\rho_{\rm b}}{\partial X}\frac{{\rm d}X}{{\rm d}t}\right)\end{aligned}$$

and similarly for $M_{\rm v}$. Combining the above equations yields a characteristic equation of the form.

$$a_1 \frac{\mathrm{d}L}{\mathrm{d}t} + a_2 \frac{\mathrm{d}T}{\mathrm{d}t} + a_3 \frac{\mathrm{d}X}{\mathrm{d}t} = a_4$$

With the a_i coefficients given by:

$$a_1 = A(\rho_\mathrm{b} - \rho_\mathrm{v})$$

$$\alpha_2 = A\left(L_\mathrm{v} \frac{\partial \rho_\mathrm{v}}{\partial T} + L\left(1 + \frac{\partial \mathrm{BPE}}{\partial T}\right) \frac{\partial \rho_\mathrm{b}}{\partial T}\right)$$

$$a_3 = AL\left(\frac{\partial \rho_\mathrm{b}}{\partial X} + \frac{\partial \mathrm{BPE}}{\partial X} \frac{\partial \rho_\mathrm{b}}{\partial T}\right)$$

$$a_4 = W_\mathrm{feed} + W_{\mathrm{b},i-1} - W_\mathrm{v} - W_\mathrm{b}$$

7.3. Conservation of energy gives

Conservation of energy for the brine, apor and heat exang lumps:

$$\frac{\mathrm{d}(M_\mathrm{b} h_\mathrm{b})}{\mathrm{d}t} = Q_\mathrm{e} + W_\mathrm{feed} h_\mathrm{feed} + W_{\mathrm{b},i-1} h_{\mathrm{b},i-1} - W_\mathrm{v} h_\mathrm{v} - W_\mathrm{b} h_\mathrm{b} - \frac{\mathrm{d}(M_\mathrm{v} h_\mathrm{v})}{\mathrm{d}t}$$

$$\frac{\mathrm{d}(M_\mathrm{v} h_\mathrm{v})}{\mathrm{d}t} = (W_{\mathrm{v,hx}} + W_{\mathrm{b,hx}} - W_\mathrm{v}) h_\mathrm{v}$$

$$\frac{\mathrm{d}(M_\mathrm{hx} h_\mathrm{hx})}{\mathrm{d}t} = 0 = W_\mathrm{st}(h_\mathrm{st} - h_\mathrm{d}) - Q_\mathrm{e}$$

Again, performing the substitution of $M = \rho AD$ as above, a similar characteristic equation is found with coefficients:

$$a_5 = A(h_\mathrm{b} \rho_\mathrm{b} - h_\mathrm{v} \rho_\mathrm{v})$$

$$\alpha_6 = A\left(L_\mathrm{v}\left(\rho_\mathrm{v} \frac{\mathrm{d}h_\mathrm{v}}{\mathrm{d}T} + h_\mathrm{v} \frac{\partial \rho_\mathrm{v}}{\partial T}\right) + L\left(1 + \frac{\partial \mathrm{BPE}}{\partial T}\right)\left(\rho_\mathrm{b} \frac{\partial h_\mathrm{b}}{\partial T} + h_\mathrm{b} \frac{\partial \rho_\mathrm{b}}{\partial T}\right)\right)$$

$$a_7 = AL\left(\rho_\mathrm{b}\left(\frac{\partial h_\mathrm{b}}{\partial X} + \frac{\partial \mathrm{BPE}}{\partial X} \frac{\partial h_\mathrm{b}}{\partial T}\right) + h_\mathrm{b}\left(\frac{\partial \rho_\mathrm{b}}{\partial X} + \frac{\partial \mathrm{BPE}}{\partial X} \frac{\partial \rho_\mathrm{b}}{\partial T}\right)\right)$$

$$a_8 = Q_\mathrm{e} + W_\mathrm{feed} h_\mathrm{feed} + W_{\mathrm{b},i-1} h_{\mathrm{b},i-1} - W_\mathrm{v} h_\mathrm{v} - W_\mathrm{b} h_\mathrm{b}$$

7.4. Conservation of species

We assume that the vapour is pure fluid and hence does not contain any salt. Therefore, conservation of species can only be expressed for the brine lump and gives:

$$\frac{\mathrm{d}(M_\mathrm{b} X_\mathrm{b})}{\mathrm{d}t} = W_\mathrm{feed} X_\mathrm{feed} + W_{\mathrm{b},i-1} X_{\mathrm{b},i-1} - W_\mathrm{b} X_\mathrm{b}$$

From this, the final characteristic equation is derived with coefficients:

$$a_9 = A \rho_\mathrm{b} X_\mathrm{b}$$

$$\alpha_{10} = ALX_\mathrm{b}\left(1 + \frac{\partial \mathrm{BPE}}{\partial T}\right) \frac{\partial \rho_\mathrm{b}}{\partial T}$$

$$a_{11} = AL\left(\rho_\mathrm{b} + X_\mathrm{b}\left(\frac{\partial \rho_\mathrm{b}}{\partial X} + \frac{\partial \mathrm{BPE}}{\partial X} \frac{\partial \rho_\mathrm{b}}{\partial T}\right)\right)$$

$$a_{12} = W_\mathrm{feed} X_\mathrm{feed} + W_{\mathrm{b},i-1} X_{\mathrm{b,i}-1} - W_\mathrm{b} X_\mathrm{b}$$

The above can then be summarized as the following system of equations:

$$\begin{bmatrix} a_1 & a_2 & a_3 \\ a_5 & a_6 & a_7 \\ a_9 & a_{10} & a_{11} \end{bmatrix} \begin{pmatrix} \mathrm{d}L/\mathrm{d}t \\ \mathrm{d}T/\mathrm{d}t \\ \mathrm{d}X/\mathrm{d}t \end{pmatrix} = \begin{pmatrix} a_4 \\ a_8 \\ a_{12} \end{pmatrix}$$

The above system of equations is implemented in Matlab. The solution procedure is as follows: the temperatures and levels of each effect are assumed to be known from measurements as a function of time. The time derivatives are evaluated using a central difference scheme. Additionally, the feed water temperature, flow rate and salinity are given. Finally, an initial guess for the brine salinity of each effect must be provided. The system of equations can then be solved for the unknown parameters brine flow rate, vapor flow rate and effect salinity.

The methodology developed above is generic in that it can be adapted for any feed water configuration, forward, backward or parallel. In the present work, a FF configuration is used. In this configuration, the brine from the previous effect is used as the feed for the next effect. Therefore, the term $W_{\mathrm{b},i-1}$ does not appear in the above equations, and the feed conditions for each effect are taken from the brine conditions calculated for the previous effect. Similarly to a PF configuration, the steam input conditions to each effect are taken from the calculated vapour conditions of the previous effect.

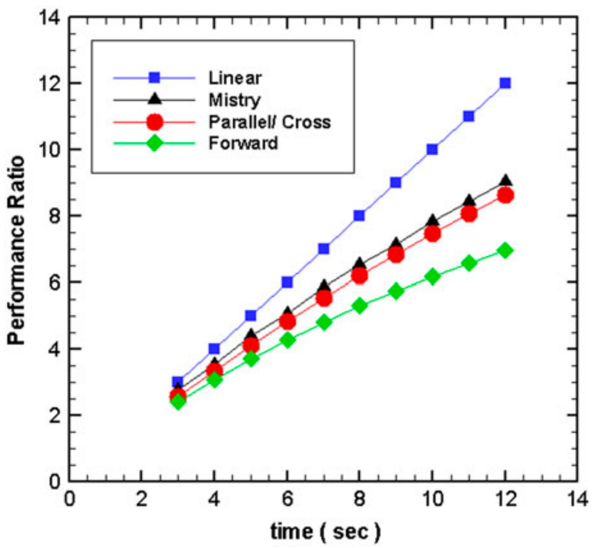

Fig. 6. Prediction of PR as a function of number of effects for forward and PF configurations.

In Fig. 6, the performance ratio (PR) of FF- and PF-MED configurations as a function of the number of effects as predicted by the model under steady conditions is presented. The assumptions are a constant production of water and a constant recovery ratio (RR) of 0.5, with a feed water salinity of 35 g/kg and temperature of 35℃, a top-brine temperature of 70℃ and the final effect temperature of 45℃, with a linear temperature drop between effects. The additional benefit of adding effects decreases as more effects are added, as shown by the inclusion of the 1:1 linear curve in the plot.

Also, the PF configuration has a higher PR as compared to the FF configuration, due to the increase in salinity of the brine used as feed water. The results of the model of Mistry [31] are also presented for a qualitative agreement, as the assumptions for producing the curve are slightly different.

8. Results

Figs. 7 and 8 present the experimental results from two different heat input conditions (Q_{e3}, Q_{e4}) when operating with two effects. As it has been stated, the aim was to maintain a constant PR of the system for about 600 s. In order to achieve that, we regulated the brine flow from first effect to the second one and also the brine of the second effect to the disposal tank, in order to keep a constant brine pool level within both vessels. The PR of the unit is presented in y axes. The outcome of the model is also presented, with a good agreement in the predicted values observed.

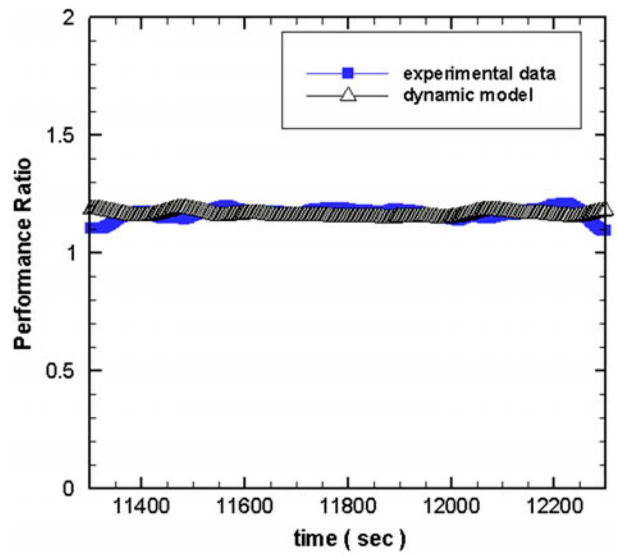

Fig. 7. Comparison of the experimental PR values with the PR values predicted by the dynamic model for heat load Q_{e2}.

It can be seen that for a given time series the dynamic model accurately predicts the magnitude and variations in the PR for every time step of this time series. As shown in both Figs. 7 and 8 for two different heat loads and time duration of 900 and 600 s, respectively, the model predictions capture accurately the experimental findings. More detailed, the dynamic model calculates the PR with an accuracy of about 90–95% most of the times. This additional improvement

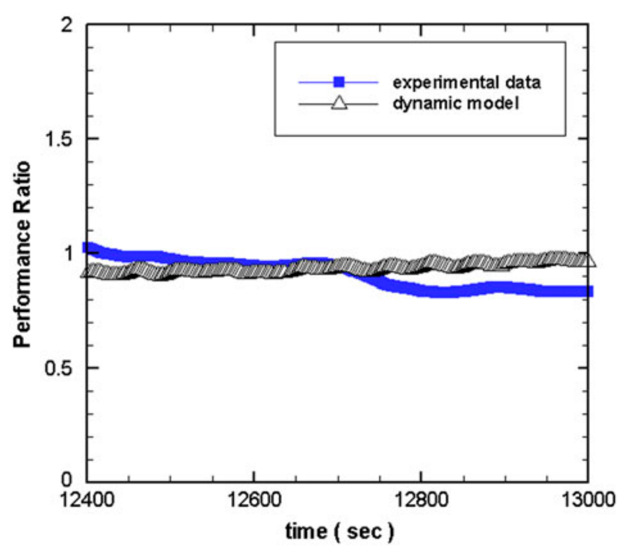

Fig. 8. Comparison of the experimental PR values with the PR values predicted by the dynamic model for heat load Q_{e3}.

in the accuracy of the dynamic model is caused by the additional assumptions taken into consideration. More precisely the additional assumption that the thermophysical properties are taken as function of temperature and salinity, helped in the improvement of the calculations, since the thermophycial properties are no longer a constant value used for any case.

Additionally apart from the PR of the unit, the model was then used to predict the performance of a 4 effect FF-MED unit with transient input conditions. Two cases were considered: in the first case—Case A—a decrease of 25% in the thermal input was applied assuming that it was caused by a decrease in the solar energy available to the plant [32], whereas in the second case—Case B—the same decrease in thermal input was applied but the feed water flow rate was also adjusted so as to achieve the same PR in a given amount of time.

As mentioned above, in Case A, a decrease of 25% to the thermal input to the plant was applied in the form of a step function. Each effect's temperature and level was considered to remain constant, while the brine salinity varied as a result of the applied step change. The model was initialized from steady conditions with a PR of 2.5 and a RR of 0.37 and the response is shown in Fig. 8. Due to the step change in thermal input, the PR also dropped instantly by 16% to 2.1 however it does not attain immediately a steady value.

As it is shown in Fig. 9, the PR of the unit started gradually to decrease from the first effect to the fourth effect. The PR value of the first effect was higher than the PR value of the rest effects and as we kept on adding more effects to the unit the PR value continued to decrease. This was expected due to the fact that the amount of steam generated by evaporation in every additional effect is less that the amount in the previous one, due to the increase in latent heat of vaporization caused by the decrease in the effect's temperature. Therefore, the amount of vapour produced by boiling is less than the amount of condensation steam used for heating in the next one.

The time needed in order for the system to reach steady-state conditions is better indicated in the salinity plots (salinity of brine produced by each effect), as shown in Fig. 10. It is clearly presented that the time constant to reach steady state is in the order of 4,000 s for the fourth effect, whereas the first effect reaches steady state after only 1,000 s. As it has been already explained, the procedure takes place gradually from the first to the last effect, thus the time lag between the effects was expected.

In Case B, the same decrease of 25% to the thermal input is applied, but now we investigate the control of the plant by setting the objective to achieve the same PR within 30 min of the step change in thermal input, as shown in Fig. 11. A linear change in feed water flow rate was applied over the desired 30 min period,

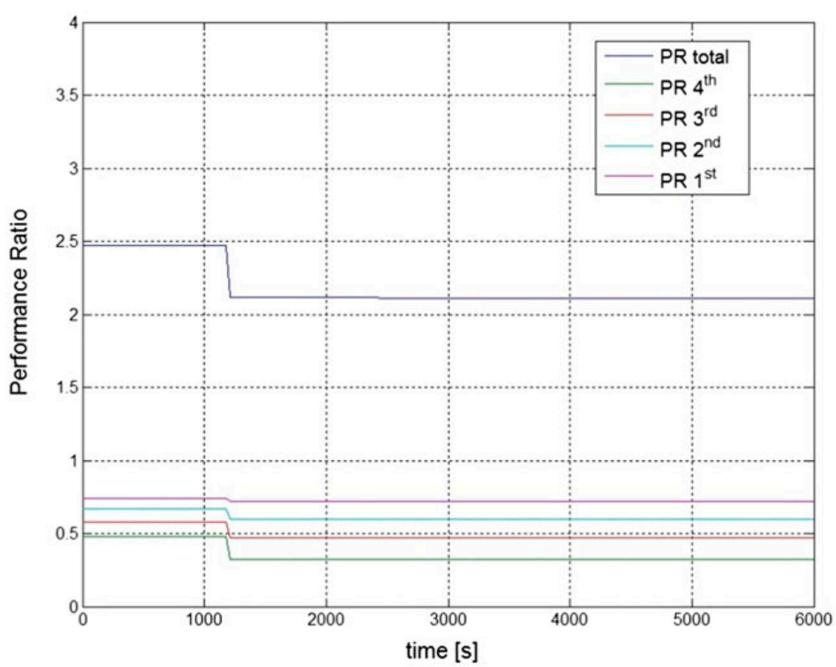

Fig. 9. System response to a 25% step reduction in thermal input, as a function of PR.

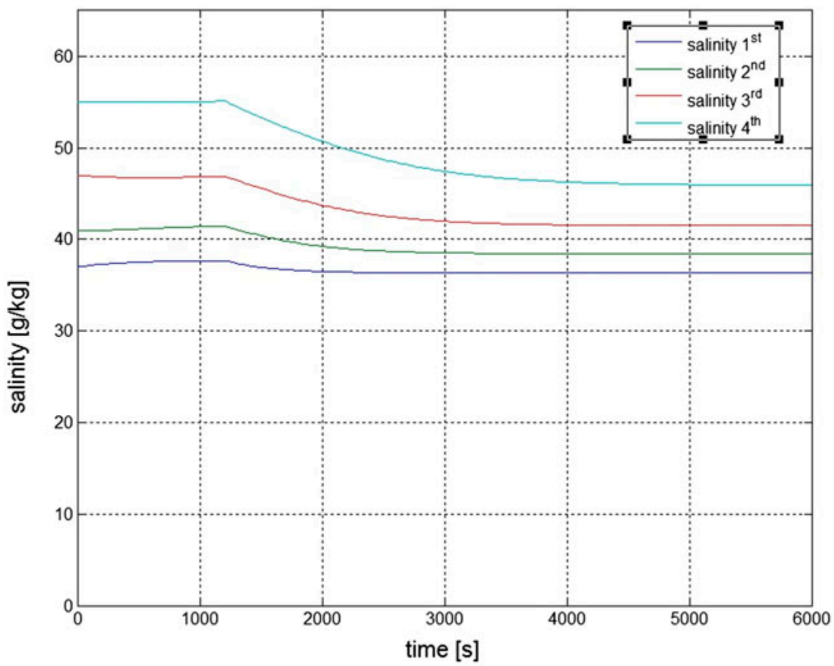

Fig. 10. System response to a 25% step reduction in thermal input as a function of salinity.

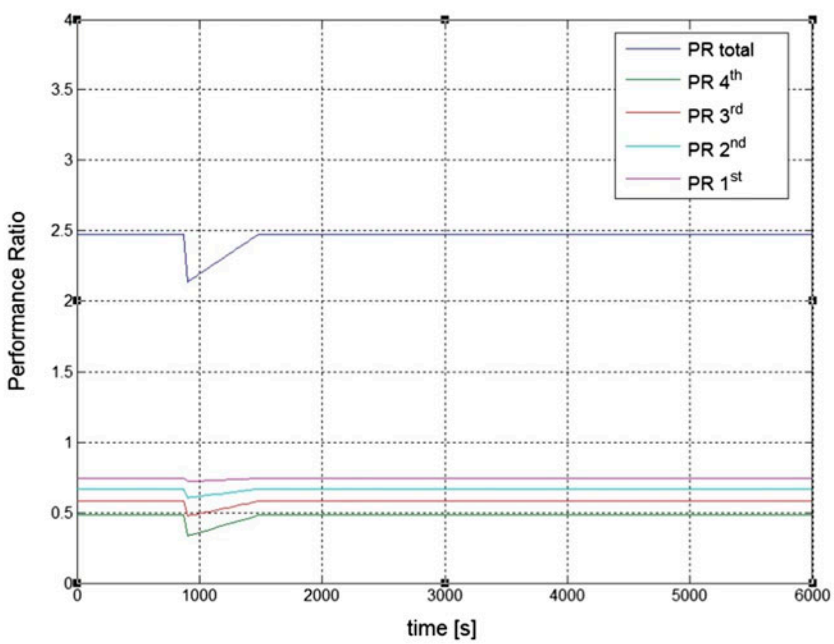

Fig. 11. System response to a 25% step reduction in thermal input as a function of PR, over the desired time period.

decreasing the flow rate also by 25% in order to achieve the same PR.

The response of the brine flow rates between effects are presented in Fig. 12. The outcome is interesting: immediately after the decrease in thermal input, brine flow rates increase, as less energy is available for the evaporation of the feed-water. Once though the feed flow rate starts to decrease, the brine flow rates also decrease until a steady state is reached. With this simple example the control of the plant is demonstrated based on the desired output.

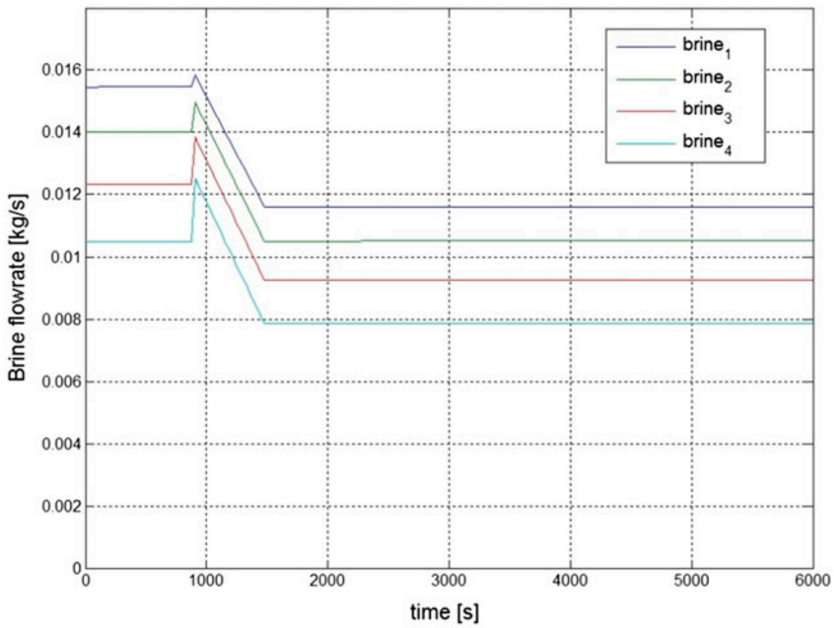

Fig. 12. System response to a 25% step reduction in thermal input as a function of brine flow rate over the desired time period.

A step function was used in order to simulate the reduction in the heat load fed to the system. This caused another limitation of the model since it could predict a decrease in the heat load similar as the one occurred during the experiments.

9. Conclusions

In the present paper, we develop a transient model for PF- and FF-MED configurations and validate it against steady state measurements of a custom MED unit. This work was the intermediate step between the steady state operation of the unit that it has been already examined, and the transient behaviour of the unit, which is to be concluded. The predictions of the model agree well with those observed experimentally, in terms of PR and brine flow rates, but also qualitatively agree with trends reported by other researchers in the literature.

The objective is to use the model to predict the performance of the MED unit when it is coupled with an intermittent renewable energy source such as solar energy, and to aid in decisions regarding plant operation and control under unsteady conditions.

References

[1] M. Elimelech, W. Phillip, The future of seawater desalination: Energy, technology, and the environment, Science 333 (2011) 712–717.
[2] M. Georgiou, A. Bonanos, J. Georgiadis, Evaluation of a solar powered distillation unit as a mitigation to water scarcity and climate change in Cyprus, Desalin. Water Treat. 57(5) (2016) 2325–2335.
[3] S.A. Kalogirou, Concentrating Solar Power Plants for Electricity and Desalinated Water Production, in Solar Thermal Applications (STH), Linkoping, 2011.
[4] S.A. Kalogirou, Seawater desalination using renewable energy sources, Prog. Energy Combust. Sci. 31 (2005) 242–281.
[5] V. Belessiotis, E. Delyannis, Water shortage and renewable energies (RE) desalination—Possible technological applications, Desalination 139 (2001) 133–138.
[6] A.M. El-Nashar, Cogeneration for power and desalination—State of the art review, Desalination 134 (2001) 7–28.
[7] V.K. Sethie, M. Pande, P. Shukla, Concentrating solar power, seawater desalination, parabolic troughs, Fresnel systems, Int. J. Adv. Renewable Energy Res. 1 (2012) 167–171.
[8] M. Darwish, Cogeneration power—Desalination plants, Desalination 69 (1988) 27–46.
[9] M. Al-Shammiri, M. Safar, Multi-effect distillation plants: State of the art, Desalination 126 (1999) 45–59.
[10] M. Darwish, Feed water arrangements in a multi-effect desalting system, Desalination 228 (2008) 30–54.
[11] H.T. El-Dessouky, H.M. Ettouney, F. Mandani, Performance of parallel feed multiple effect evaporation system for seawater desalination, Appl. Therm. Eng. 20 (2000) 1679–1706.
[12] M. Georgiou, A. Bonanos, J. Georgiadis, Experimental evaluation of a multiple-effect distillation unit in low seawater flow conditions, Desalin. Water Treat. 55(12) (2014) 3267–3276.

[13] Y. El-Sayed, R. Silver, Fundamentals of Distillation, in Principles of Desalination, Academic Press, New York, NY, 1980, pp. 55–109.
[14] M. Darwish, H. Abdulrahim, Feed water arrangements in a multi-effect desalting system, Desalination 228 (2008) 30–54.
[15] M. Darwish, F. Al-Juwayhel, H. Abdulraheim, Multi-effect boiling systems from an energy viewpoint, Desalination 194 (2006) 22–39.
[16] P. Druetta, P. Aguirre, S. Mussati, Optimization of multi-effect evaporation desalination plants, Desalination 311 (2013) 1–15.
[17] O. Hamed, Thermal assessment of a multiple effect boiling (MEB) desalination system, Desalination 86 (1992) 325–339.
[18] N. Aly, A. El-Figi, Thermal performance of seawater desalination systems, Desalination 158 (2003) 127–142.
[19] M. El-Allawy, Predictive Simulation of the Performance of MED/TVC Desalination Distiller, in IDA World Congress, International Desalination Association, Bahamas, 2003.
[20] R. Kamali, S. Mohebinia, Experience of design and optimization of multi-effects desalination systems in Iran, Desalination 222 (2008) 639–645.
[21] M. Ameri, S. Mohammadi, M. Hosseini, M. Seifi, Effect of design parameters on multi-effect desalinationsystem specifications, Desalination 245 (2009) 266–283.
[22] N. Aly, M. Marwan, Dynamic response of multi-effect evaporators, Desalination 114 (1997) 189–196.
[23] G. Kishore, A. Raha, A. Adak, V. Srivastava, Steady- and transient-state analysis of a multi-effect mechanical vapour compression desalination plant, Int. J. Nucl. Desalin. 2 (2006) 117–131.
[24] L. Roca, L. Yebra, M. Berenguel, A. De La Calle, Dynamic modeling and simulation of a multi-effect distillation plant, in Proceedings of 9th International Modelica Conference, Munich, 2012.
[25] A. de la Calle, J. Bonilla, L. Roca, P. Palenzuela, Dynamic modeling and simulation of a solar-assisted multi-effect distillation plant, Desalination 357 (2015) 65–76.
[26] A. de la Calle, J. Bonilla, L. Roca, P. Palenzuela, Dynamic modeling and performance of the first cell of a multi-effect distillation plant, Appl. Therm. Eng. 70 (2014) 410–420.
[27] N.M. Aly, M.A. Marwan, Dynamic response of multi-effect evaporators, Desalination 114 (1997) 189–196.
[28] D. Kumar, V. Kumar, V. Singh, Modeling and dynamic simulation of mixed feed multi-effect evaporators in paper industry, Appl. Math. Modell. 37 (2013) 384–397.
[29] M. Mazini, A. Yazdizadeh, M. Ramezani, Dynamic modeling of multi-effect desalination with thermal vapor compressor plant, Desalination 353 (2014) 98–108.
[30] M. Sharqawy, J.H. Lienhard, S. Zubair, Thermophysical properties of seawater: A review of existing correlations and data, Desalin. Water Treat. 16 (2010) 354–380.
[31] K. Mistry, M.A. Antar, J.H. Lienhard V, An improved model for multiple effect distillation, Desalin. Water Treat. 51 (2013) 807–821.
[32] M.C. Georgiou, A.M. Bonanos, J.G. Georgiadis, Evaluation of a multiple-effect distillation unit under partial load operating conditions, in Hindawi Publishing Corporation Conference Papers in Energy, Cairo, 2013.